EMBO reports

scientific report

Calcium tips the balance: a microtubule plus end to lattice binding switch operates in the carboxyl terminus of BPAG1n4

Mridu Kapur, Wei Wang, Michael T. Maloney, Ivan Millan, Victor F. Lundin, Thuy-An Tran & Yanmin Yang[+]
Department of Neurology and Neurological Sciences, Stanford University School of Medicine, Stanford, California, USA

Microtubules (MTs) are integral to numerous cellular functions, such as cell adhesion, differentiation and intracellular transport. Their dynamics are largely controlled by diverse MT-interacting proteins, but the signalling mechanisms that regulate these interactions remain elusive. In this report, we identify a rapid, calcium-regulated switch between MT plus end interaction and lattice binding within the carboxyl terminus of BPAG1n4. This switch is EF-hand dependent, and mutations of the EF-hands abolish this dynamic behaviour. Our study thus uncovers a new, calcium-dependent regulatory mechanism for a spectraplakin, BPAG1n4, at the MT plus end.

Keywords: spectraplakin; microtubule plus end; calcium; EF-hand

EMBO *reports* (2012) **13,** 1021–1029. doi:10.1038/embor.2012.140

INTRODUCTION

Microtubule (MT)-associated proteins (MAPs) and plus end-binding proteins (+TIPs) have a principal role in modulating the organization and dynamic behaviour of MTs. +TIPs not only regulate the growth and shrinkage of MTs [1,2], but also their attachment to other cellular structures [3]. Disruption of these interactions has been linked to many human diseases [4–6]. So far, phosphorylation is the most well-known mechanism for controlling MT-interacting proteins, and it has been implicated in the spatial and cell-cycle-dependent regulation of many MAPs and +TIPs [7–10]. Despite these insights, the potential exists for more signals that modulate the rapid coordination of this dynamic interaction system, yet their discovery has remained elusive.

BPAG1n4, a 600-kDa neuronal protein is a member of the spectraplakin family, which includes ACF-7 in mammals, and shot and *Vab-10* in invertebrates. Spectraplakins can bind to actin and intermediate filaments as well as MTs, making them master coordinators of the cytoskeleton [11–14]. BPAG1n4 has an essential role in retrograde axonal transport in sensory neurons, by virtue of functional domains that associate with the $p150_{Glued}$ dynactin complex and with retrolinkin, an endosomal receptor [11,15]. In addition, on the basis of sequence homology, the C-terminus of BPAG1n4 might contain MT-binding sites [10,16–18].

In this study, we identify an extremely rapid mechanism for switching between MT plus end and lattice-binding activities in the C-terminus of BPAG1n4. This regulation is EF-hand and calcium (Ca^{2+}) dependent. Alteration of Ca^{2+} responsiveness, resulting from mutations in the EF-hands, completely abolishes the rapid switch while rendering permanent the binding interaction with either the MT lattice or the plus end. This newly identified, Ca^{2+}-dependent regulatory mechanism in spectraplakins might have a critical role in a number of diverse MT-associated processes. We thus provide the first evidence for a mechanism through which Ca^{2+} can directly and rapidly regulate the dynamic interaction of MTs with a key regulatory protein.

RESULTS AND DISCUSSION

BP4tail preferentially binds to the plus end

The MT-binding domain (MTBD) at the C-terminus of BPAG1n4 consists of a Gas2-related segment [10,11,16] (supplementary Fig S1 online). Consistent with its sequence, green fluorescent protein (GFP)-MTBD decorated the MT network when expressed in Cos-7 cells (supplementary Fig S2A online; supplementary video 1 online, $n>30$ cells). Notably, downstream of the MTBD, the C-terminus harbours a short Sx-IP homology motif that might constitute an EB1-binding domain (EBBD) [17,18]. Using an *in vitro* binding assay, we showed that EBBD could directly bind to EB1 (supplementary Fig S2D online), with a binding affinity of $4.5 \pm 0.74\,\mu M$ (± s.d., $n=3$, supplementary Fig S2E online). The EB1 family is a central player at the plus end, responsible for the localization of many +TIPs [19]. In Cos-7 cells, GFP-EBBD robustly tracked the plus end, mimicking the behaviour of an EB1 family member, EB3 (supplementary Fig S2B,C online; supplementary video 1 online, $n>30$). The velocity of EBBD tip tracking ($0.392 \pm 0.01\,\mu m/s$, ± s.e.m., $n=5$ cells) was similar to

Department of Neurology and Neurological Sciences, Stanford University School of Medicine, MSLS Building, Room P259, 1201 Welch Road, Stanford, California 94305, USA
[+]Corresponding author. Tel: +1 650 736 1032; Fax: +1 650 498 6262;
E-mail: yyanmin@stanford.edu

Received 10 May 2012; revised 28 August 2012; accepted 28 August 2012; published online 21 September 2012

Fig 1 | A Ca^{2+}-regulated rapid switch between MT plus end and lattice association. (**A**) Cos-7 cell expressing GFP-BP4tail. Inset; magnified boxed region. Comet position; red arrow ($t = 0$ s), green arrowhead ($t = 6$ s) and blue arrowhead ($t = 12$ s). Colour overlay images (red; $t = 0$ s, green; $t = 6$ s and blue; $t = 12$ s on the extreme right. Scale bar, 10 μm. (Supplementary Video 1 online). (**B,B′**) GFP-BP4tail changes localization in response to ionomycin. A representative Cos-7 cell expressing GFP-BP4tail (**B**) before and (**B′**) 30 s after ionomycin addition. Ionomycin was added at $t = 0$ s. Inset right, magnified boxed region showing frames at 4 s intervals. Red arrow = original comet position ($t = -8/30$ s), red arrowheads mark subsequent positions. Scale bar, 10 μm (supplementary Video 2 online). (**C**) Representative linescans plotting the normalized distribution of GFP-BP4tail along the MT, before (green) and 30 s after (red) addition of ionomycin. The graph represents the average normalized intensity (± s.e.m.) of 10–15 individual MTs from the cell in (**B,B′**), plotted against distance from the MT end. Fluorescence was normalized to the average fluorescence intensity of the cell, such that average fluorescence equalled 1. (**D–F**) $n = 15$ cells, 10–15 MTs per cell, Student's paired t-test. (**D**) Ionomycin treatment causes a significant decrease in GFP-BP4tail fluorescence at the MT tip ($^*P < 0.05$, ± s.e.m.). (**E**) Ionomycin treatment causes a significant increase in GFP-BP4tail fluorescence along the MT lattice ($^{**}P < 0.01$, ± s.e.m.). (**F**) GFP-BP4tail redistributes after ionomycin treatment. Ratio of normalized fluorescence at MT tip (0–2 μm) to that at MT lattice (3–5 μm) before and 30 s after ionomycin ($^{**}P < 0.01$). (**G**) *In vitro* pull-down assays using purified MBP-EB1 and Flag-BP4tail. 2 mM Ca^{2+} decreases the binding of Flag-BP4tail to MBP-EB1 (lane 5 versus lane 4), $n > 3$, ± s.e.m., $^*P < 0.05$. (**H**) Co-sedimentation of BP4tail with polymerized MTs. High Ca^{2+} results in a trend towards increased binding of Flag-BP4tail to MTs (lane 5 versus lane 4), $n > 3$, ± s.e.m., $P = 0.07$. GFP, green fluorescent protein; MT, microtubule.

that observed for EB3 (0.352 ± 0.03 μm/s, $n = 5$), and falls within the range documented for other +TIPs [20].

Our findings demonstrate that the C-terminus of BPAG1n4 has two independent MT-interaction domains, one that underlies interaction with the MT lattice (MTBD) and the other that mediates association with the plus end through binding with EB1 family proteins (EBBD).

Although certain proteins such as CLASP2 and *Drosophila* msps also contain both MT lattice and EB1-binding sites, the interaction of these proteins with MTs is spatially regulated, and they interact either with the lattice or the plus end in the cell interior versus periphery [7,21]. It is important to consider how these two different binding activities within the same short C-terminus stretch of BPAG1n4 co-function without impeding one another.

To understand the behaviour of the C-terminus of BPAG1n4, we expressed a construct spanning both the MTBD and the EBBD (BP4tail, supplementary Fig S1 online). We found that despite containing the MTBD, GFP-BP4tail localized predominantly to plus ends (Fig 1A; supplementary video 1 online, $n > 30$ cells) and tracked them with a velocity of 0.418 ± 0.01 μm/s ($n = 5$), behaviour similar to that of EBBD alone. This suggests that the lattice-binding activity of the MTBD is suppressed in the context of BP4tail, leading us to question how the preferential interaction with MT plus ends is determined. We hypothesized that an active regulatory mechanism might underlie this selective interaction.

Ca^{2+}-regulated switch from plus end to MT lattice

In a search for candidate regulatory mechanisms, we analysed the sequence of our expression construct, noting two Ca^{2+}-binding EF-hand motifs immediately upstream of the MTBD (domain structure in supplementary Fig S1 online). Their proximity to both the MTBD and EBBD prompted us to consider that Ca^{2+} might have a role in controlling binding selectivity of the C-terminus of BPAG1n4. To investigate this possibility, we treated Cos-7 cells expressing GFP-BP4tail (EF-MTBD-EBBD) with the Ca^{2+} ionophore, ionomycin, to induce an increase in the cytosolic Ca^{2+} levels. Before treatment, GFP-BP4tail preferentially localizes to comets at MT plus ends and shows tip-tracking behaviour (Fig 1A,B). Fluorescence intensity linescan analysis verified that BP4tail forms a 2–3 μm long comet at the MT tip, similar to the reported localization of EB1 (Fig 1C, $n = 15$ cells) [17]. Remarkably, following ionomycin treatment, we observed a striking translocation of BP4tail from the plus ends to the MT lattice, and both comet localization and tip tracking were mostly abolished (Fig 1B,B′; supplementary video 2 online, $n = 15$). This switch could occur as quickly as 10 s, and overall was completed 30–40 s after treatment (supplementary Video 2 online). To obtain quantitative evidence, we conducted linescan analysis before and 30 seconds after ionomycin treatment. This analysis revealed a decrease of fluorescence at the MT tip (0–2 μm, Fig 1D, $P < 0.05$), accompanied by an increase in fluorescence along the lattice (3–5 μm, Fig 1E, $P < 0.01$), indicating that high Ca^{2+} might alter the binding preference of BP4tail, resulting in its redistribution along the MT (Fig 1E, $P < 0.01$). These results demonstrate that BP4tail undergoes a switch between plus end and lattice binding in response to elevated Ca^{2+} levels.

To obtain more support, we examined the effect of Ca^{2+} on the binding of Flag-BP4tail to purified maltose binding protein (MBP)-EB1 *in vitro* (Fig 1G). We found that 2 mM Ca^{2+} significantly inhibited the binding of BP4tail to EB1 ($P < 0.05$, $n > 3$, Fig 1G). We next assessed whether Ca^{2+} could alter the interaction between BP4tail and MTs. Polymerized MTs were incubated with Flag-BP4tail in either 0 or 2 mM Ca^{2+} buffer, and then MTs and any bound proteins were co-sedimented. Although not statistically significant ($P = 0.09$, $n > 3$, Fig 1H), a clear trend indicates that increased MT binding by BP4tail occurs at 2 mM Ca^{2+}. Together, these *in vitro* results indicate that Ca^{2+} regulation might act more strongly at the EB1-binding site, which might be sufficient to cause the observed switch. They support our *in vivo* finding that the interaction between BP4tail and EB1/MTs is Ca^{2+} dependent.

The MTBD is essential for the Ca^{2+}-regulated switch

We hypothesized that Ca^{2+} binding to the EF-hands might underlie the observed regulation. To test this, we assessed whether Ca^{2+} could directly alter MT structure or EB1-binding sites. We examined the behaviour of GFP-EB3 and GFP-EBBD (without EF-hands). Both proteins track the MT plus end after ionomycin treatment (Fig 2A–D), indicating that the observed switch of BP4tail from MT tips to lattice in response to elevated Ca^{2+} is unlikely to be a result of structural changes or of a redistribution of EB1 family proteins. Next, we deleted the MTBD from BP4tail, creating an EF-EBBD construct (supplementary Fig S1 online). Like BP4tail, GFP-EF-EBBD tracked MT plus ends; yet, despite the

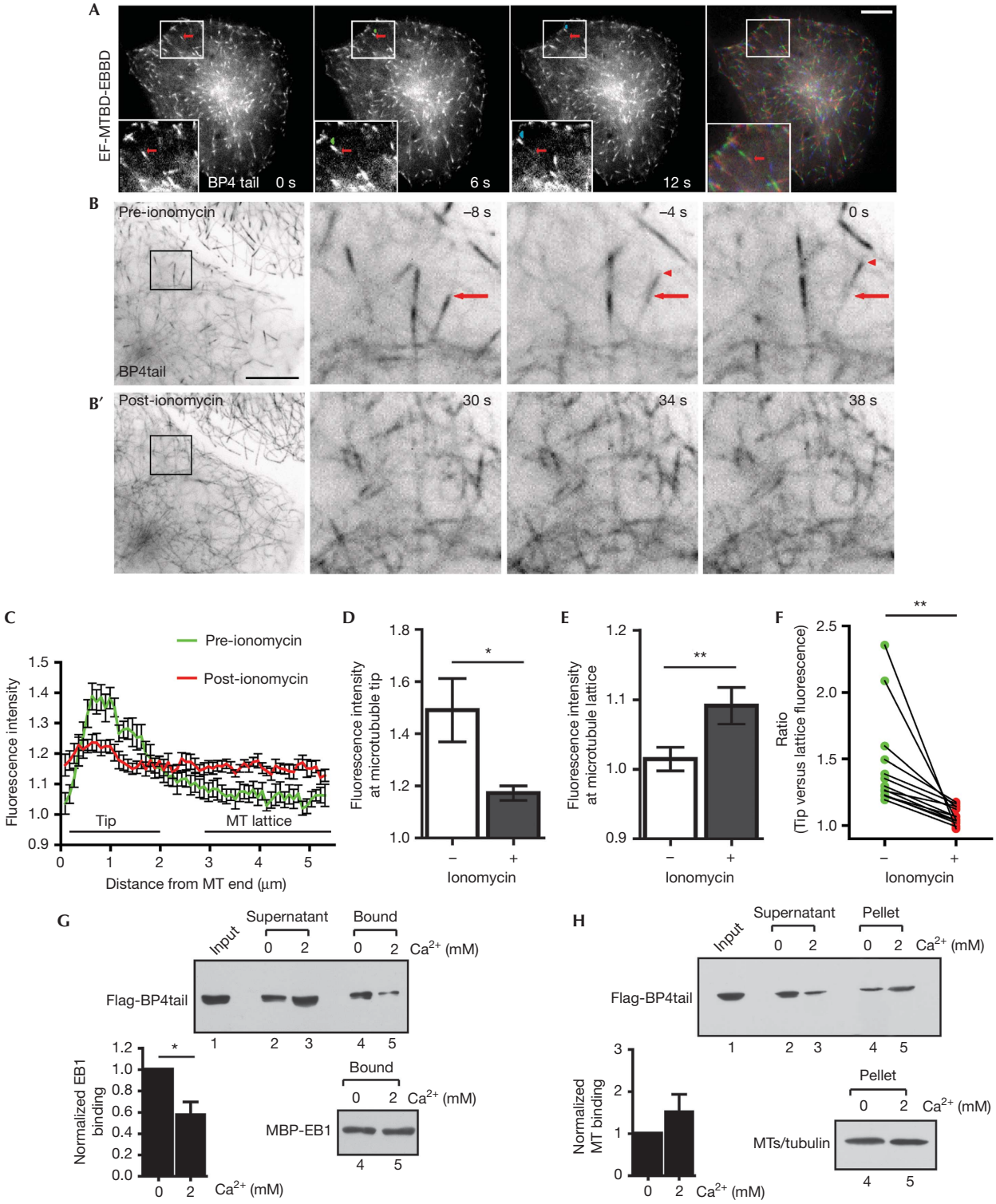

presence of EF-hands, it remained unresponsive to ionomycin (Fig 2E–F; supplementary video 3 online, $n=10$). Linescan measurements taken before and 30 s after ionomycin treatment show no change in the tip localization of EF-EBBD (Fig 2F, $n=10$), and EF-EBBD continues to tip track for several minutes after treatment. Together, these data demonstrate that increased Ca^{2+} does not change EF-EBBD-specific binding activity at the plus end, and that the switch of BP4tail from the MT tip to the lattice requires the MTBD. Finally, as the presence of the MTBD appears essential for the switch from the plus end to the lattice, we examined the effect of increased Ca^{2+} on the localization of the MTBD. Both GFP-MTBD (Fig 2H) and GFP-EF-MTBD share similar lattice binding

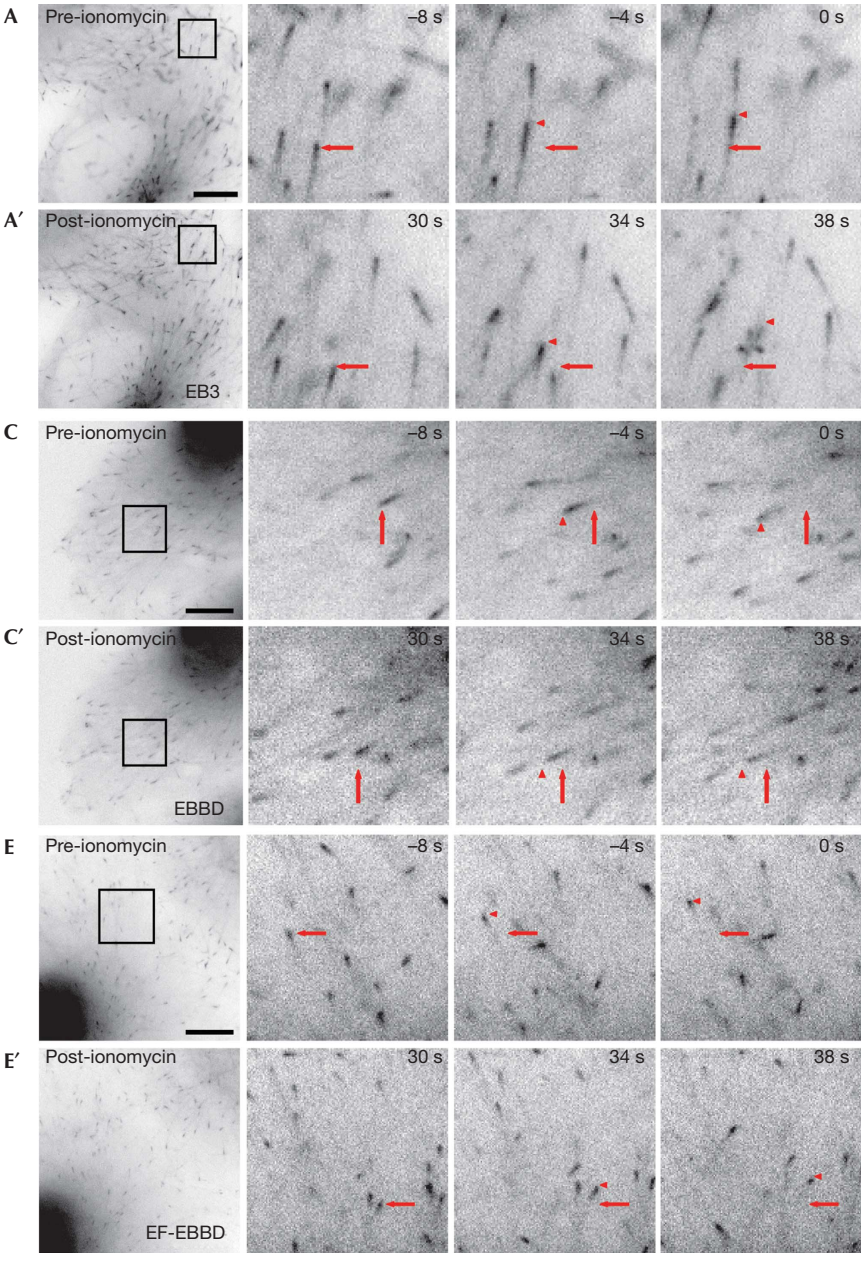

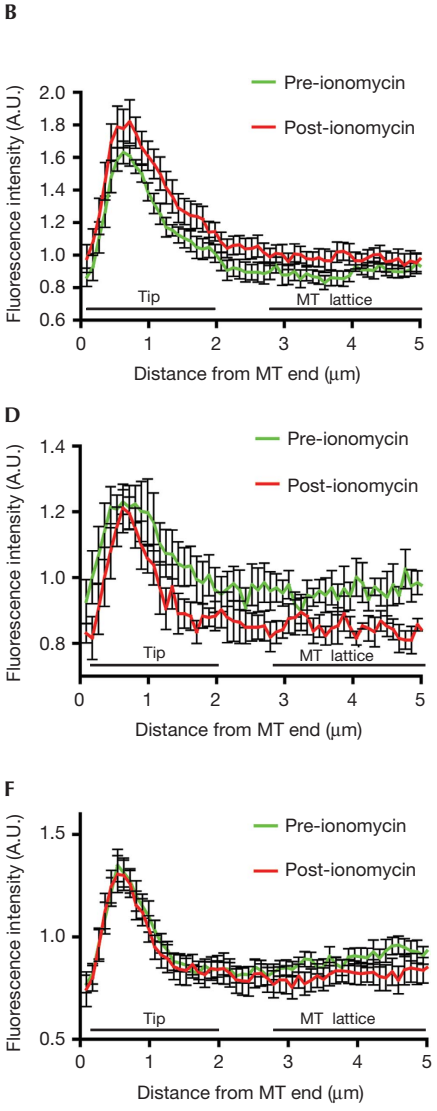

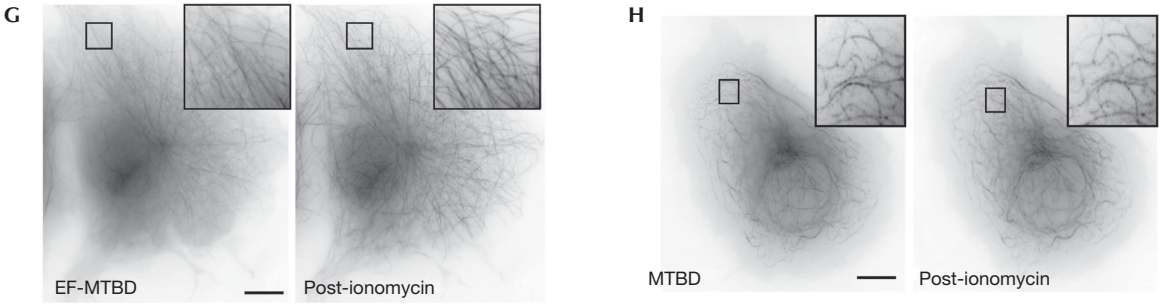

◀ **Fig 2** | The MTBD is essential for the Ca^{2+}-regulated switch. Addition of ionomycin does not affect the tip tracking of **(A,A′)** EB3; **(C′,C′)** EBBD and **(E,E′)** EF-EBBD. Representative Cos-7 cells expressing GFP-EB3, GFP-EBBD and GFP-EF-EBBD **(A,C,E)** before and **(A′,C′,E′)** 30 s after ionomycin addition. Ionomycin was added at $t = 0$ s. Inset right, magnified boxed region showing frames at 4 s intervals. Red arrow = original comet position ($t = -8/30$ s), red arrowheads mark subsequent positions. Scale bar, 10 μm. **(E,E′)** corresponds to supplementary Video 3 online. **(B,D,F)** Representative linescans plotting the normalized distribution of **(B)** GFP-EB3, **(D)** GFP-EBBD and **(F)** GFP-EF-EBBD along the MT, before (green) sand 30 s after (red) addition of ionomycin (10–15 MTs, ± s.e.m.). **(G)** GFP-EF-MTBD localizes to MTs before and after the addition of ionomycin. Inset = magnified boxed region. Scale bar, 10 μm (supplementary Video 4 online). **(H)** Addition of ionomycin has no effect on GFP-MTBD-labelled MTs. Inset = magnified boxed region. Scale bar, 10 μm. EBBD, EB1-binding domain; GFP, green fluorescent protein; MT, microtubule; MTBD, MT-binding domain.

before and after ionomycin treatment (Fig 2G; supplementary video 4 online, $n = 10$). Our data demonstrate that in order for the Ca^{2+}-driven switch to be functional, both lattice and plus end-binding domains have to be present.

Suppression of lattice binding requires EF-hands

To define the role of the EF-hands in the Ca^{2+}-regulated switch, we deleted both EF-hand motifs from BP4tail (ΔEF). GFP-BP4tail ΔEF localized exclusively to the MT lattice (Fig 3A, $n > 30$). Similar to the effect of deletion, when three conserved Ca^{2+}-binding aspartate residues in both EF-hands were replaced by alanine (Fig 3E), the mutated BP4tail (EF1,2MUT) mimicked the localization of BP4tail ΔEF, binding to the lattice with no observable plus end tracking (Fig 3B, $n > 30$). We then further dissected the role of each EF-hand by introducing mutations in one hand at a time. We found that mutations in EF-hand 1 (BP4tail EF1MUT) also resulted in lattice localizatin (Fig 3C, $n > 20$). In contrast, when EF-hand 2 was mutated (BP4tail EF2MUT), the mutant protein maintained specific association with the plus end, making it the only EF-hand mutant to retain the +TIP behaviour of the wild-type BP4tail construct at basal Ca^{2+} levels (Fig 3D, $n > 20$). These results strongly suggest that the condition of the two EF-hands determine the selective interaction of BP4tail with the MT plus ends versus the lattice.

Supporting evidence was gained from co-immunoprecipitation experiments in which Flag-EB1 was co-transfected in HEK cells with GFP-BP4tail or its mutants (supplementary Fig S3A online). GFP-BP4tail, but not GFP alone, was co-precipitated by Flag antibody. However, the co-precipitation of BP4tail by Flag-EB1 was impaired by deletion or mutation of both EF-hands (ΔEF, EF1,2MUT), or mutation of only EF-hand 1 (EF1MUT). Consistent with our live-imaging data, mutations in EF-hand 2 (EF2MUT) did not strongly affect the interaction of BP4tail with EB1. The immunoprecipitation was performed in a Ca^{2+}-free environment, suggesting again that the condition of the EF-hands can directly affect BP4tail-binding activity, even in the absence of Ca^{2+}.

Importantly, we found that mutation of the EF-hands had no major effect on the behaviour of EF-MTBD or EF-EBBD, which retain their localization to the MT lattice and plus end, respectively (supplementary Fig S4A,B online, $n = 10$). Thus, although mutation of EF-hands can drastically alter the localization of BP4tail, their regulatory effect requires the presence of both the MTBD and the EBBD.

The Ca^{2+}-regulated rapid switch is EF-hand dependent

As mutation of the EF-hands can affect the preferential localization of BP4tail, we questioned whether they also altered BP4tail's ability to rapidly switch localization in response to increased Ca^{2+}. To address this, we repeated the live-imaging and ionomycin experiments using the EF-hand mutants of BP4tail. As expected, mutation of both EF-hands (EF1,2MUT) or of EF-hand 1 (EF1MUT), which result in lattice binding under basal condition, also abolish any Ca^{2+} sensitivity, and their localization along MTs remained unaltered by ionomycin treatment (Fig 4A–B′, $n = 10$). Remarkably, when we examined BP4tail EF2MUT, we found that its plus end localization was completely insensitive to ionomycin treatment (Fig 4C–G; supplementary video 5 online). Like EF-EBBD (supplementary Video 3 online), BP4tail EF2MUT continued to track the plus end, without any change in activity for minutes after ionomycin treatment. The fluorescent intensity at the tip and at the lattice remained unchanged on treatment (Fig 4E–F, $n = 10$, $P > 0.05$). Thus, although the tip-tracking behaviour of wild-type BP4tail and EF2MUT are alike, the inability of EF2MUT to switch from the plus end to the lattice on ionomycin treatment strongly suggests that a functional EF-hand 2 is required for this rapid switch.

Consistent with our live-imaging data, mutation of the EF-hands abolishes the Ca^{2+} regulation previously observed for wild-type BP4tail *in vitro*. Increased Ca^{2+} has no significant effect on the interaction of EF2MUT with EB1 ($P > 0.05$, $n > 3$, Fig 4H). Similarly, the co-sedimentation of EF1MUT with MTs is unaltered by high Ca^{2+} ($P > 0.05$, $n > 3$, Fig 4I). As expected, the interaction between EF1,2MUT and EB1 or MTs was also insensitive to high Ca^{2+} ($P > 0.05$, $n > 3$, Fig 4H,I). Thus, functional EF-hands are essential for the observed Ca^{2+} regulation.

A hypothetical model of the Ca^{2+}-regulated switch

Taken together, our data uncover a new, Ca^{2+}-regulated dynamic interaction of the C-terminus of BPAG1n4 with the MT plus end and lattice. We demonstrate that the EF-hands underlie the Ca^{2+} regulation of this preferential interaction. Here, we propose a model of the Ca^{2+}-regulated switch (Fig 5).

In the absence of the EF-hands, BP4tail localizes to the MT lattice (Fig 3A,B). Similar behaviour has been observed in *Drosophila* shot, in which the homologous domain, lacking the upstream EF-hands, was found to decorate the lattice [22]. However, when functional EF-hands are present, Ca^{2+} binding might alter the domain conformation to modulate the selectivity of the two binding activities. At basal or 0 mM Ca^{2+} levels, the proposed 'closed' conformation of BP4tail with the two EF-hands present might suppress the functional activity of the MTBD, preventing lattice interaction and leading to a preferential association with EB1 at plus ends (Fig 1A). When Ca^{2+} levels increase, Ca^{2+} binding to the EF-hands might modify the domain to its 'open' conformation, exposing the MTBD-binding site, leading to the observed rapid switch in localization (Fig 1B,B′; supplementary video 2 online). Mutation of EF-hand 1 led to lattice binding, strongly suggesting that EF-hand 1 might have

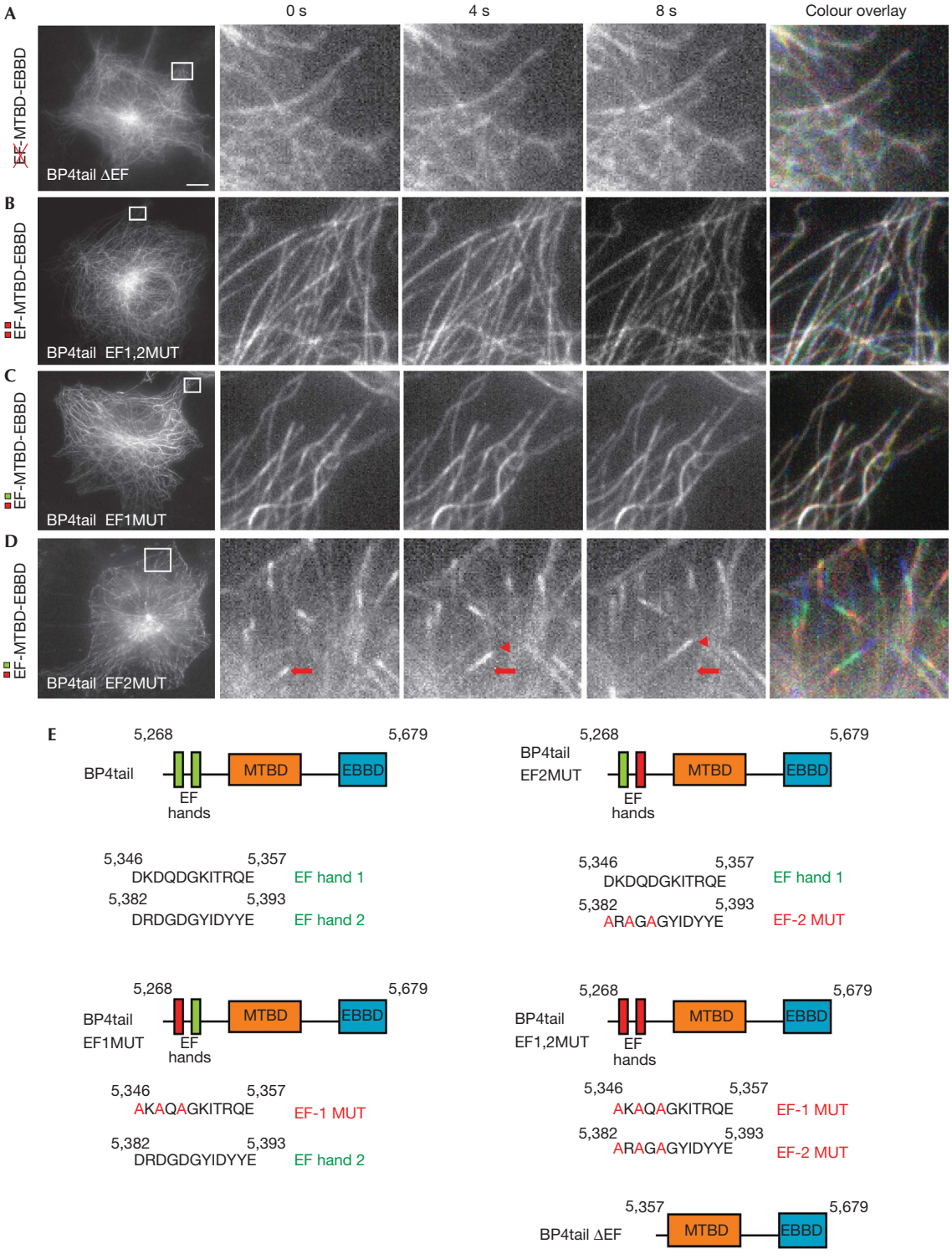

Fig 3 | The suppression of lattice interaction requires the EF-hands. Cos-7 cells expressing **(A)** BP4tail ΔEF, **(B)** BP4tail EF1,2MUT, **(C)** BP4tail EF1MUT and **(D)** BP4tail EF2MUT. Red arrow = comet position ($t = 0$ s), red arrowheads mark subsequent positions ($t = 4$ s and $t = 8$ s). Coloured overlay images (red; $t = 0$ s, green; $t = 4$ s and blue; $t = 8$ s) on the extreme right. Schematic of the domain structure and mutations shown on left of each image. Scale bar, 10 μm. **(E)** Domain structure of BP4tail and EF-hand mutants. EBBD, EB1-binding domain; MTBD, MT-binding domain.

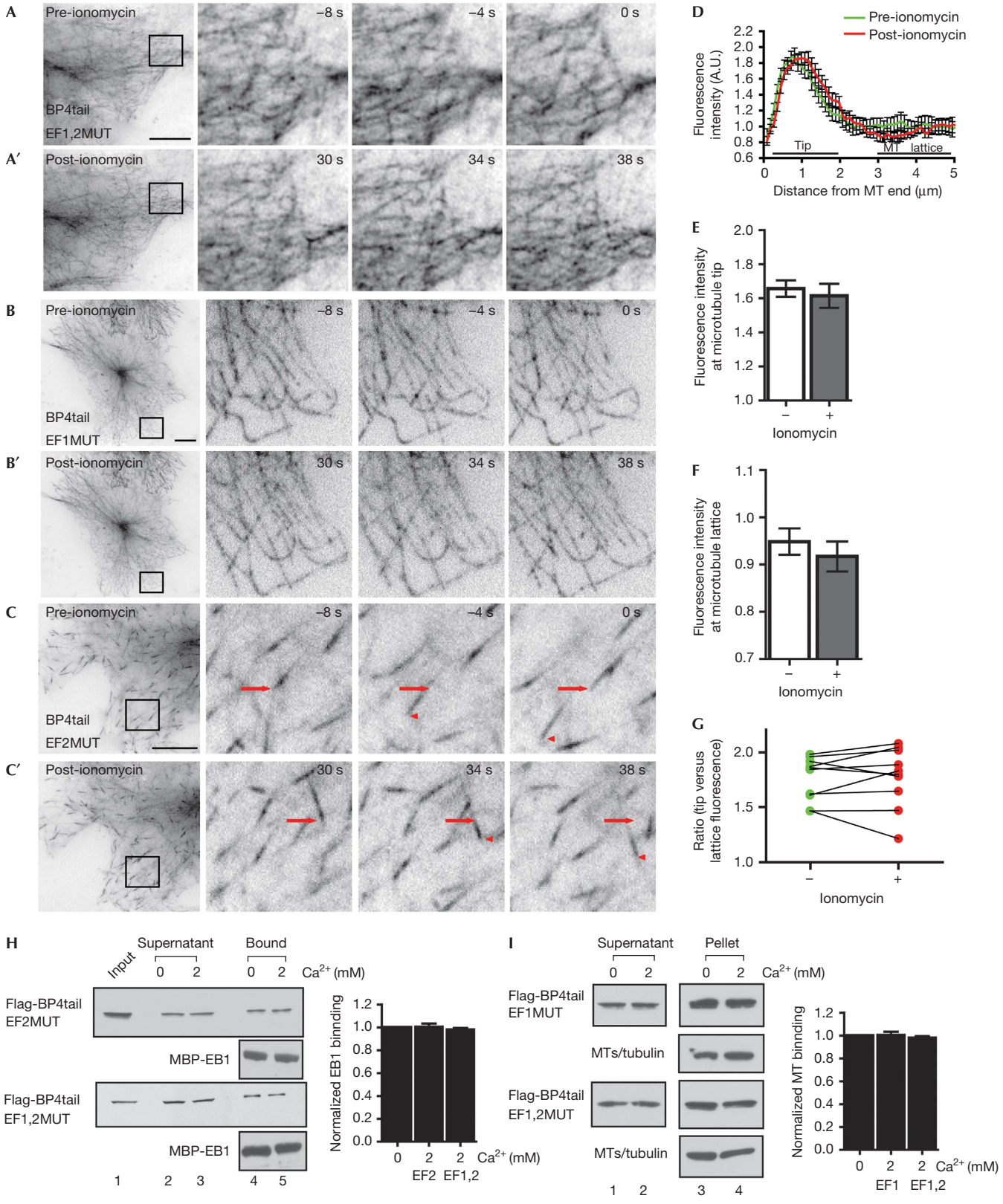

Fig 4 | For caption see next page.

◀ **Fig 4** | The Ca^{2+}-regulated rapid switch from plus end to lattice binding is EF-hand dependent. Addition of ionomycin does not affect the localization of **(A,A′)** BP4tail EF1,MUT, **(B,B′)** BP4tail EF1MUT or **(C,C′)** BP4tail EF2MUT. Representative Cos-7 cells expressing GFP-BP4tail EF1,2MUT, EF1MUT or EF2MUT **(A,B,C)** before and **(A′,B′,C′)** 30 s after ionomycin addition. Ionomycin was added at $t = 0$ s. Inset right, magnified boxed region showing frames at 4 s intervals. **(C,C′)** Red arrow = original comet position ($t = -8/30$ s), red arrowheads mark subsequent positions. Schematic of the domain structure and mutation shown on left of each image. Scale bar, 10 μm. **(C,C′)** corresponds to supplementary Video 5 online. **(D)** Representative linescans plotting the normalized distribution of GFP-BP4tail EF2MUT along the MT, before (green) and 30 s after (red) addition of ionomycin. (10–15 MTs, ± s.e.m., cell shown in **C,C′**). **(E–G)** $n = 10$ cells, 10–15 individual MTs per cell, Student's paired *t*-test. **(E)** Ionomycin treatment does not alter GFP-BP4tail EF2MUT fluorescence at the MT tip ($P > 0.05$, ± s.e.m.). **(F)** Ionomycin treatment does not change GFP-BP4tail EF2MUT fluorescence along the MT lattice ($P > 0.05$, ± s.e.m.). **(G)** Ratio of normalized fluorescence at MT tip (0–2 μm) to that at the lattice (3–5 μm) before and 30 s after ionomycin ($P > 0.05$). **(H)** *In vitro* pull-down between EF-hand mutants of BP4tail and MBP-EB1. High Ca^{2+} does not significantly alter the interaction with EB1 (lane 5 versus lane 4). $n > 3$, ± s.e.m., $P > 0.05$. **(I)** Co-sedimentation of the EF-hand mutants of BP4tail with polymerized MTs. High Ca^{2+} does not alter the binding to MTs (lane 4 versus lane 3). $n > 3$, ± s.e.m., $P > 0.05$. GFP, green fluorescent protein; MT, microtubule.

a role in suppressing the MTBD activity (Fig 3C). In contrast, EF-hand 2 appears more important for the release of MTBD suppression following an increase in cytosolic Ca^{2+}. Disruption of EF-hand 2 locked BP4tail EF2MUT in a 'closed' conformation, retaining all the + TIP features of wild-type BP4tail, even under high Ca^{2+} conditions (Fig 4C,C′; supplementary video 5 online). It is apparent that Ca^{2+} binding to EF-hand 1 alone is not sufficient to release the suppression of lattice interaction. Thus, the Ca^{2+}-regulated switch is exquisitely sensitive to disruption of the EF-hands and requires both EF-hands to be present and functional.

While Ca^{2+} has been implicated in the regulation of MT dynamics through MAPs and + TIPs, it usually acts upstream of or directly on a kinase [23–25]. Although STIM1 is a + TIP that contains EF-hands, its association with EB1 does not seem to be directly Ca^{2+} regulated [26]. Our study presents the first evidence of Ca^{2+} directly and rapidly modulating the interaction of a protein at the plus end, uncovering a new mechanism through which Ca^{2+} signalling can directly regulate the dynamic interactions of MTs with regulatory proteins. This process might have an essential role in many cellular activities, including cellular adhesion, differentiation and axonal transport.

Like other spectraplakins, BPAG1n4 is a massive protein, containing several functional domains. At the ultrastructural level, BPAG1n4 mainly localizes to vesicles along MTs [11], suggesting that its interaction with the plus end might be dynamic and transient. Future investigations must overcome technical hurdles to examine the Ca^{2+} regulation of full-length BPAG1n4. The conservation of the C-terminal domain of BPAG1n4 in other members of the spectraplakin family, such as ACF7, *shot* and *Vab-10*, suggests that Ca^{2+} regulation of the plus end interaction might have a vital role in their functional activities as well [27]. Addressing the potential role of this Ca^{2+} switch might be crucial to fully understanding spectraplakins' many diverse functions.

METHODS

Ionomycin treatment. Cos-7 cells were imaged in extracellular solution containing 2 mM $CaCl_2$ under perfusion. Cells were

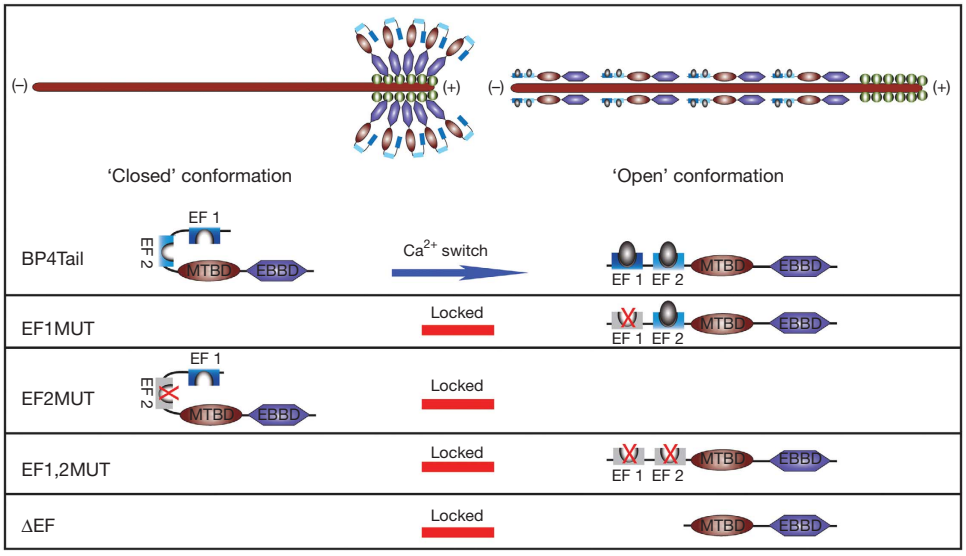

Fig 5 | A hypothetical model of the Ca^{2+} switch. Model of the Ca^{2+}-regulated switch in BP4tail. In the 'closed' conformation, lattice binding is suppressed allowing + TIP binding, while in the 'open' conformation lattice binding is dominant (upper). Wild-type BP4tail undergoes a transition from closed to open conformation in the presence of high Ca^{2+}, EF2MUT remains locked in the closed conformation, while all other constructs (EF1MUT, EF1,2MUT and ΔEF) remain locked in the open conformation (lower). EBBD, EB1-binding domain; MTBD, MT-binding domain.

imaged for 1–2 min after the addition of ionomycin (2 μM), acquiring one frame every 2 s.

Linescan analysis. Analysis was performed using MetaMorph v7.7. Briefly, 10–15 individual MTs were analysed before and 30 s after the addition of ionomycin. Fluorescence measurements were normalized to the average fluorescence of the cell (average fluorescence = 1). The effect of ionomycin was determined using a paired Student's *t*-test.

EB1-binding assay. MBP-EB1 was immobilized on amylose beads and used to pull down Flag-BP4tail (wild-type/mutants) from HEK cell lysate in buffer containing either 0 or 2 mM $CaCl_2$. Equivalent volumes of the supernatant and bound fractions were processed for immunoblotting. The Flag signal was normalized to MBP, and EB1 binding was calculated by dividing the intensity of the bound band by the summed intensities of the supernatant and bound bands. Binding at 2 mM Ca^{2+} was expressed as a fraction of binding in the absence of Ca^{2+} ($n>3$, *t*-test).

MT co-sedimentation. A modified *in vivo* co-sedimentation assay was used (BK038, Cytoskeleton). HEK cells transfected with Flag-BP4tail (wild-type/mutants) were treated with nocodazole to depolymerize MTs, and then lysed and processed to acquire the Flag protein and the soluble tubulin pool. MTs were then repolymerized by taxol, and subjected to co-sedimentation by standard protocols. The results were quantified as described above ($n>3$, *t*-test). For details, see supplementary methods online.

Supplementary information is available at EMBO *reports* online (http://www.emboreports.org).

ACKNOWLEDGEMENTS

We would like to thank A. Akhmanova and W.J. Nelson for kindly sharing constructs. We also thank S. Kim and C. Garner for assistance with live imaging. This work was supported by grants from the National Institutes of Health (NIH R01), March of Dimes foundation, Stanford BioX fellowship (T.-A.T.) and Stanford Graduate fellowship (M.K.), Human Frontiers Science Programme (V.F.L.).

Author contributions: M.K. and Y.Y. conceived the study, designed the experiments and M.K., Y.Y. and M.T.M. wrote the manuscript. M.K. carried out all experiments and analysis, M.T.M. assisted with the live imaging, and W.W., T.-A.T., I.M. and V.F.L. assisted with the biochemistry. Y.Y. supervised the work. All authors discussed results and commented on the manuscript.

CONFLICT OF INTEREST

The authors declare that they have no conflict of interest.

REFERENCES

1. Tirnauer JS, Bierer BE (2000) EB1 proteins regulate microtubule dynamics, cell polarity, and chromosome stability. *J Cell Biol* **149:** 761–766
2. Al-Bassam J, Kim H, Brouhard G, van Oijen A, Harrison SC, Chang F (2010) CLASP promotes microtubule rescue by recruiting tubulin dimers to the microtubule. *Dev Cell* **19:** 245–258
3. Pierre P, Scheel J, Rickard JE, Kreis TE (1992) CLIP-170 links endocytic vesicles to microtubules. *Cell* **70:** 887–900
4. Ding J *et al* (2006) Gene targeting of GAN in mouse causes a toxic accumulation of microtubule-associated protein 8 and impaired retrograde axonal transport. *Hum Mol Genet* **15:** 1451–1463
5. Garcia ML, Cleveland DW (2001) Going new places using an old MAP: tau, microtubules and human neurodegenerative disease. *Curr Opin Cell Biol* **13:** 41–48
6. Green RA, Wollman R, Kaplan KB (2005) APC and EB1 function together in mitosis to regulate spindle dynamics and chromosome alignment. *Mol Biol Cell* **16:** 4609–4622
7. Kumar P, Lyle KS, Gierke S, Matov A, Danuser G, Wittmann T (2009) GSK3beta phosphorylation modulates CLASP-microtubule association and lamella microtubule attachment. *J Cell Biol* **184:** 895–908
8. Ban R, Matsuzaki H, Akashi T, Sakashita G, Taniguchi H, Park SY, Tanaka H, Furukawa K, Urano T (2009) Mitotic regulation of the stability of microtubule plus-end tracking protein EB3 by ubiquitin ligase SIAH-1 and Aurora mitotic kinases. *J Biol Chem* **284:** 28367–28381
9. Zhou F-Q, Zhou J, Dedhar S, Wu Y-H, Snider WD (2004) NGF-induced axon growth is mediated by localized inactivation of GSK-3beta and functions of the microtubule plus end binding protein APC. *Neuron* **42:** 897–912
10. Wu X, Shen QT, Oristian DS, Lu CP, Zheng Q, Wang HW, Fuchs E (2011) Skin stem cells orchestrate directional migration by regulating microtubule-ACF7 connections through GSK3β. *Cell* **144:** 341–352
11. Liu J-J, Ding J, Kowal AS, Nardine T, Allen E, Delcroix JD, Wu C, Mobley W, Fuchs E, Yang Y (2003) BPAG1n4 is essential for retrograde axonal transport in sensory neurons. *J Cell Biol* **163:** 223–229
12. Wu X, Kodama A, Fuchs E (2008) ACF7 regulates cytoskeletal-focal adhesion dynamics and migration and has ATPase activity. *Cell* **135:** 137–148
13. Röper K, Brown NH (2003) Maintaining epithelial integrity: a function for gigantic spectraplakin isoforms in adherens junctions. *J Cell Biol* **162:** 1305–1315
14. Bosher JM, Hahn BS, Legouis R, Sookhareea S, Weimer RM, Gansmuller A, Chisholm AD, Rose AM, Bessereau JL, Labouesse M (2003) The Caenorhabditis elegans vab-10 spectraplakin isoforms protect the epidermis against internal and external forces. *J Cell Biol* **161:** 757–768
15. Liu J-J, Ding J, Wu C, Bhagavatula P, Cui B, Chu S, Mobley WC, Yang Y (2007) Retrolinkin, a membrane protein, plays an important role in retrograde axonal transport. *Proc Natl Acad Sci USA* **104:** 2223–2228
16. Sun D, Leung CL, Liem RK (2001) Characterization of the microtubule binding domain of microtubule actin crosslinking factor (MACF): identification of a novel group of microtubule associated proteins. *J Cell Sci* **114:** 161–172
17. Slep KC, Rogers SL, Elliott SL, Ohkura H, Kolodziej PA, Vale RD (2005) Structural determinants for EB1-mediated recruitment of APC and spectraplakins to the microtubule plus end. *J Cell Biol* **168:** 587–598
18. Honnappa S *et al* (2009) An EB1-binding motif acts as a microtubule tip localization signal. *Cell* **138:** 366–376
19. Dixit R, Barnett B, Lazarus JE, Tokito M, Goldman YE, Holzbaur EL (2009) Microtubule plus-end tracking by CLIP-170 requires EB1. *Proc Natl Acad Sci USA* **106:** 492–497
20. Stepanova T, Slemmer J, Hoogenraad CC, Lansbergen G, Dortland B, De Zeeuw CI, Grosveld F, van Cappellen G, Akhmanova A, Galjart N (2003) Visualization of microtubule growth in cultured neurons via the use of EB3-GFP (end-binding protein 3-green fluorescent protein). *J Neuro* **23:** 2655–2664
21. Currie JD, Stewman S, Schimizzi G, Slep KC, Ma A, Rogers SL (2011) The microtubule lattice and plus-end association of Drosophila mini spindles is spatially regulated to fine-tune microtubule dynamics. *Mol Biol Cell* **22:** 4343–4361
22. Applewhite DA, Grode KD, Keller D, Zadeh AD, Slep KC, Rogers SL (2010) The spectraplakin short stop is an actin – microtubule cross-linker that contributes to organization of the microtubule network. *Mol Biol Cell* **21:** 1714–1724
23. Kapitein LC, Yau KW, Gouveia SM, van der Zwan WA, Wulf PS, Keijzer N, Demmers J, Jaworski J, Akhmanova A, Hoogenraad CC (2011) NMDA receptor activation suppresses microtubule growth and spine entry. *J Neuro* **31:** 8194–8209
24. Togo T (2009) Ca(2+) regulates the subcellular localization of adenomatous polyposis coli tumor suppressor protein. *Biochem Biophys Res Commun* **388:** 12–16
25. Ohkawa N, Fujitani K, Tokunaga E, Furuya S, Inokuchi K (2007) The microtubule destabilizer stathmin mediates the development of dendritic arbors in neuronal cells. *J Cell Sci* **120:** 1447–1456
26. Grigoriev I *et al* (2008) STIM1 is a MT-plus-end-tracking protein involved in remodeling of the ER. *Curr Biol* **18:** 177–182
27. Lee S, Kolodziej P (2002) Short stop provides an essential link between F-actin and microtubules during axon extension. *Development* **129:** 1195–1204